

Improving Counterflow Detection in Dense Crowds with Scene Features

Ziyan Wu*, Richard J. Radke

Department of Electrical, Computer, and Systems Engineering, Rensselaer Polytechnic Institute, 110 8th Street, Troy, NY, USA 12180

Abstract

This paper addresses the problem of detecting counterflow motion in videos of highly dense crowds. We focus on improving the detection performance by identifying scene features — that is, features on motionless background surfaces. We propose a three-way classifier to differentiate counterflow from normal flow, simultaneously identifying scene features based on statistics of low-level feature point tracks. By monitoring scene features, we can reduce the likelihood that moving features' point tracks mix with scene feature point tracks, as well as detect and discard frames with periodic jitter. We also construct a Scene Feature Heat Map, which reflects the space-varying probability that object trajectories might mix with scene features. When an object trajectory nears a high-probability region of this map, we switch to a more time-consuming and robust joint Lucas-Kanade tracking algorithm to improve performance. We evaluate the algorithms with extensive

*Phone: +1 (518) 961-1754, Fax: +1 (518) 276-8715

Email addresses: wuz5@rpi.edu (Ziyan Wu), rjradke@ecse.rpi.edu (Richard J. Radke)

URL: www.rpi.edu/~wuz5 (Ziyan Wu), www.ecse.rpi.edu/~rjradke (Richard J. Radke)

experiments on several datasets, including almost three weeks of data from an airport surveillance camera network. The experiments demonstrate the feasibility of the proposed algorithms and their significant improvements for counterflow detection.

Keywords: counterflow, scene feature, tracking, false alarm, video surveillance

1. Introduction

Counterflow detection is a critical problem in security-related surveillance. For example, a person moving the wrong way through the exit corridor of an airport can prompt an entire terminal to be “dumped”, resulting in hundreds of delayed flights and inconvenienced passengers. By tracking low-level feature points, the typical flow direction can easily be determined. However, most of the cameras deployed in security surveillance networks have poor resolution and quality compared to a consumer digital camera, which can negatively affect tracking algorithms, especially during long-term operation. Another issue preventing automatic video analytic algorithms from replacing manual monitoring is that the false positive rate is likely to be very high compared to the small number of true positives in 24/7 continuous operation.

This paper presents three contributions. First, we demonstrate that counterflow detection can be significantly improved by introducing a novel classifier to identify scene features in the image, which are then used to mitigate cases in which foreground and background features are mixed in the same point trajectory. Second, by monitoring the statistics of scene features, we identify jitter frames that should not play a role in tracking. Third, we con-

19 struct a Scene Feature Heat Map that enables the automatic selection of a
20 suitable tracking scheme for point tracks in different locations of the image
21 to achieve more robust performance. We conducted extensive experiments
22 on both a standard dataset (CAVIAR) and several real-world video datasets
23 acquired from an airport surveillance camera network, demonstrating that
24 our counterflow detection algorithm is significantly improved by using the
25 scene-feature-based algorithms. The resulting framework was in continuous
26 operation for three weeks at a major airport, successfully detecting hundreds
27 of counterflow events with no misses and only three false alarms.

28 **2. Related Work**

29 The problem of detecting dominant motions in crowded video and classi-
30 fying outlying motions has been widely studied [8, 13, 2, 4]. Tu and Rittscher
31 [17] introduced a crowd segmentation algorithm by clustering interest points
32 into groups by determining maximal cliques in a graph. However, both the
33 algorithm and experiments are based on videos from overhead views only,
34 which is the easiest case for counterflow detection. Andrade et al. [3] pro-
35 posed an algorithm for detecting abnormal movements in crowds by applying
36 principal component analysis to optical flow maps and spectral clustering to
37 hidden Markov models, but did not perform any real-world experiments.
38 This algorithm identifies abnormal motion based on a trained flow map,
39 which is sensitive to noise and may cause false positives for normal motions
40 not covered by the training set. Brostow and Cipolla [7] used an unsupervised
41 Bayesian detection algorithm to segment low-level feature tracklets based on
42 a spatial prior and a likelihood model of coherent motion. Ali and Shah [1]

43 modeled a highly dense crowd as an aperiodic dynamical system that can be
44 studied with Lagrangian particle dynamics techniques. Antonini and Thiran
45 [4] introduced a trajectory clustering method based on independent compo-
46 nent analysis. Junejo et al. [13] applied graph cuts to segmenting tracklets.
47 Cheriyyadat and Radke [10] proposed a trajectory clustering algorithm based
48 on non-negative matrix factorization.

49 Cheriyyadat and Radke [9] proposed an automatic dominant motion de-
50 tection method by clustering trajectories based on longest common subse-
51 quences. Since individual people are difficult to segment, the inputs to the
52 algorithm are tracked low-level features obtained using optical flow. Our al-
53 gorithm takes a similar approach. However, these types of algorithms might
54 not yield good results in situations involving low-resolution cameras and poor
55 image quality. Marcenaro and Vernazza [15] proposed an image stabilization
56 algorithm based on feature tracking in which scene features are used as refer-
57 ences to compensate for the motion of the camera. In this paper, we propose
58 a classifier to identify scene features in the context of detecting counterflow
59 motion. We show that by using information from the scene features, the per-
60 formance and accuracy of foreground object point tracking can be improved
61 under low-quality, complex-background conditions.

62 An earlier version of this paper appeared in [18]. Here, a new concept, the
63 Scene Feature Heat Map, and a joint processing mechanism within a camera
64 network are proposed in order to further reduce the false alarm rate. A new
65 experiment on the CAVIAR dataset and a more extensive long-term experi-
66 ment using a camera network at an airport are presented, demonstrating the
67 effectiveness of the proposed algorithm.



Figure 1: Results of feature tracking. (a) Features detected in the image. (b) Point tracks extracted from a video sequence.

68 3. Feature Tracking

69 Even in the age of high-quality consumer digital cameras, videos from
 70 surveillance camera networks are frequently low-resolution (e.g., 352×240).
 71 Since we want the system to process video streams from tens of cameras in
 72 real time, and the dominant (or allowable) direction of motion is all we need
 73 to know, we use low-level features to track the flow. We first identify low-
 74 level features in the initial frame using the FAST corner detector [16]. The
 75 features are then tracked over time using the Kanade-Lucas-Tomasi (KLT)
 76 optical flow algorithm [14], adapting the pyramid representation in [6], which
 77 can track large pixel motions while keeping the size of the integration window
 78 relatively small.

79 The results of feature tracking are shown in Figure 1, in which red circles
 80 indicate all the features detected in the current frame (up to a maximum
 81 number, e.g., 300) and blue circles indicate reliably-trackable features. New
 82 features are added to the tracker every 5-10 frames, discarding those too close

83 to current tracks. These feature tracks form a large trajectory set.

84 4. Improving Robustness with a Scene Feature Classifier

85 This low-level feature point tracking is often inaccurate, due to both the
 86 low resolution and quality of the input videos and periodic jitter. Conse-
 87 quently, it is common for features on foreground objects (corresponding to
 88 the allowable/counter flow) to mix or merge with stationary scene features,
 89 as illustrated in Figure 2.

90 Our solution to this problem is to build a three-way classifier to identify
 91 normal flow, counterflow, and scene features. The point tracks are classified
 92 at a specified interval (e.g., every 300 frames). The recognized scene features
 93 can also be used to compensate for location drift caused by jitter. Here we
 94 assume flow goes roughly up-and-down on the image.

95 Let $\mathbf{L}^j = \{(x_j(1), y_j(1)), \dots, (x_j(n_j), y_j(n_j))\}$ be the data of the j^{th} point
 96 track. We define two features (d_1^j, d_2^j) for each trajectory \mathbf{L}^j as

$$d_1^j = \frac{1}{n_j^2} \sum_{i=1}^{\lfloor \frac{n_j}{3} \rfloor} y_j(n_j - i) - y_j(i)$$

$$d_2^j = \frac{1}{n_j} \sqrt{\sum_{i=2}^{n_j} (x_j(i) - x_j(1))^2 + (y_j(i) - y_j(1))^2}$$

97 That is, d_1^j represents the difference in sum on y between the first third and
 98 last third of the trajectory, and d_2^j represents the variance of the points on
 99 the trajectory from their initial position.

100 As Figure 3 illustrates, the three-way classifier separates trajectories cor-
 101 responding to normal flow, counterflow, and scene features based on the rule

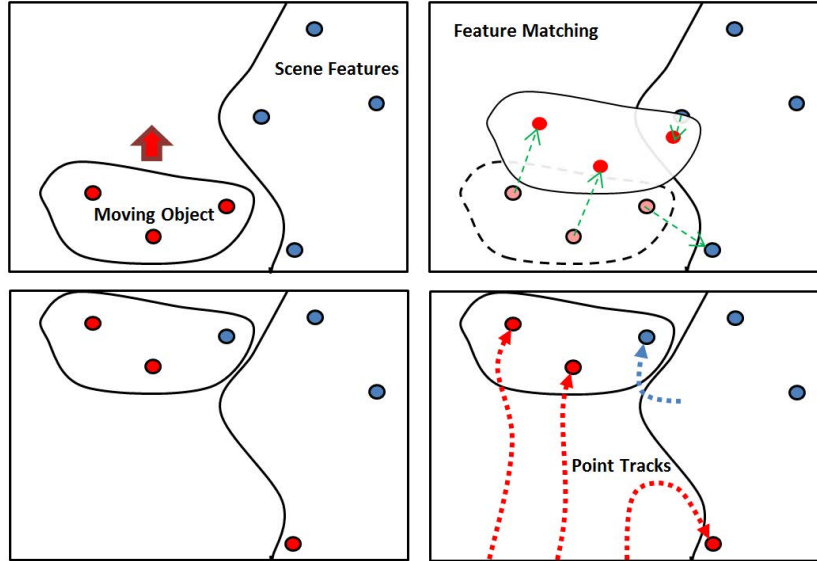


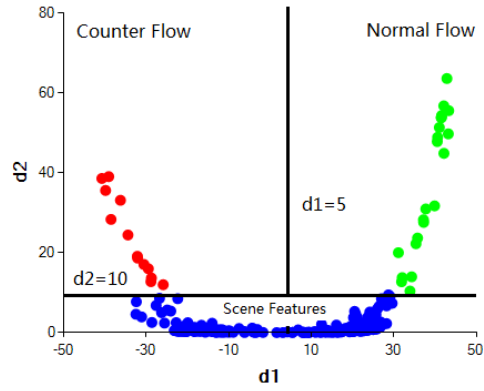
Figure 2: Foreground points mixing with scene points.

$$\mathbf{L}^j = \begin{cases} \text{normal flow} & d_1^j > a, d_2^j > b \\ \text{counterflow} & d_1^j \leq a, d_2^j > b \\ \text{scene feature} & d_2^j \leq b \end{cases} \quad (1)$$

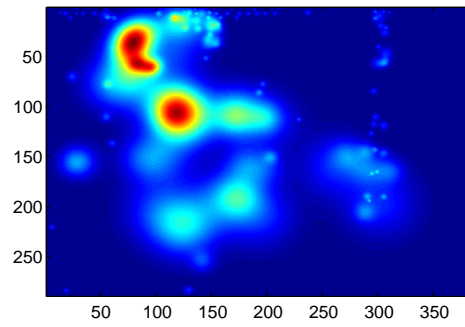
102 The value of b in the classifier to separate scene points can be obtained
 103 by learning the standard deviation in the image location of features from
 104 an image sequence containing only the background. We used $b = 10$ in our
 105 experiments. The value of a is trained on a short sequence based on user
 106 editing of missed detections and false alarms. That is, a is set to an initial
 107 value (e.g., 5) and is adjusted based on user edits to the smallest number
 108 such that the classifier has no missed detections (which are operationally
 109 extremely costly).



(a)



(b)



(c)

Figure 3: Result of the three-way classifier and Scene Feature Heat Map. (a) Feature tracks. (b) Classifier result corresponding to (a). (c) Scene Feature Heat Map corresponding to (a).

110 After the scene features are classified, they can be used to deal with
 111 two issues. First, point tracks that were classified as scene points in the
 112 previous decision are matched and tracked only after all of the other (flow)
 113 features are matched and tracked for each frame. This step significantly
 114 reduces the probability that scene features mix with moving features and
 115 confuse the tracker/classifier, as we show in Section 7. Second, the statistics
 116 of scene features provide an easy way to detect frames with jitter, as shown in
 117 Figure 4. We can easily learn a threshold on the change in x values along the
 118 trajectories for scene points that detects jitter frames. These frames are then
 119 ignored for the purposes of tracking and classification, which substantially
 120 improves robustness.

121 5. Scene Feature Heat Map

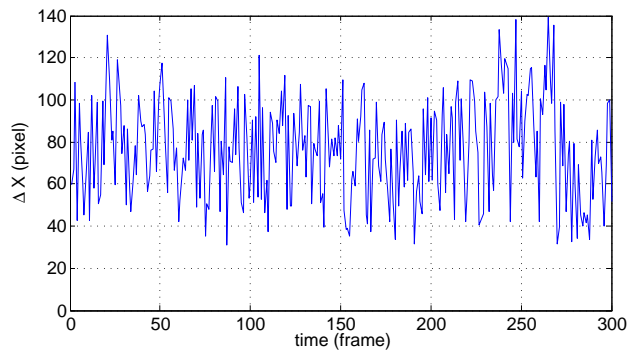
122 Using only the feature tracks classified as scene features \mathcal{S} , we generate a
 123 Scene Feature Heat Map (SFHM) to further reduce false alarms, defined as:

$$h(u, v) = \sum_{\mathbf{L}^j \in \mathcal{S}} \exp \left\{ \frac{-1}{2\sigma^2} \begin{bmatrix} u - x_j(n_j) \\ v - y_j(n_j) \end{bmatrix}^\top \Sigma^{-1} \begin{bmatrix} u - x_j(n_j) \\ v - y_j(n_j) \end{bmatrix} \right\} \quad (2)$$

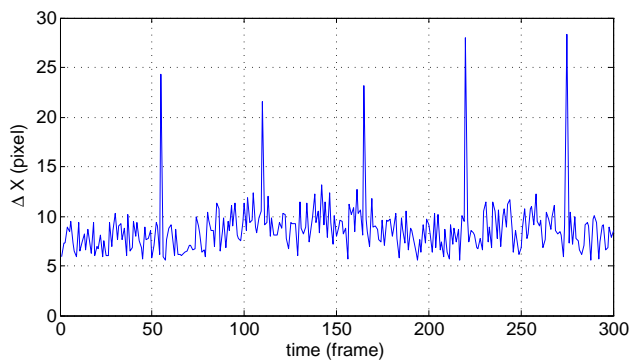
124 in which Σ is the 2×2 covariance matrix of point track data \mathbf{L}^j . σ is a scale
 125 factor depending on the image size, defined as

$$\sigma = b^{-2} \sqrt{(W^2 + H^2)} \quad (3)$$

126 in which W and H are the width and height of the image respectively. Figure
 127 3(c) shows a Scene Feature Heat Map generated from the results shown in
 128 Figure 3(a-b). The SFHM is basically a visualization of the probability that
 129 a feature track at the given pixel contains a scene feature.



(a)



(b)

Figure 4: Statistics of (a) moving points and (b) scene feature points. Jitter frames are clearly visible as spikes in (b).

130 When a tracked feature moves close to a “high-heat” region on the SFHM,
 131 it is more likely to mix with scene features. Hence, in this case, we use
 132 a Pyramidal Joint Lucas-Kanade (JLK) algorithm [5] for feature tracking,
 133 which combines the Kanade-Lucas [14] and Horn-Schunck [12] optical flow
 134 algorithms. That is, we define the overall tracking problem at a pixel as

135 minimizing C by finding the displacement $\mathbf{t} = (t_x, t_y)^\top$, in which

$$C = \begin{cases} C_{LK} & h(x, y) < \beta\sigma \\ C_{JLK} = C_{LK} + \lambda C_{HS} & \text{otherwise} \end{cases} \quad (4)$$

The two cost functions are defined as

$$C_{LK}(u, v) = \sum_{(x, y)} w(x, y) (I(x + u, y + v, t + 1) - I(x, y, t))^2$$

$$C_{HS}(u, v) = \left\| \begin{bmatrix} u \\ v \end{bmatrix} - \begin{bmatrix} \hat{u} \\ \hat{v} \end{bmatrix} \right\|^2 \quad (5)$$

136 in which $w(x, y)$ is a windowing function and $(\hat{u}, \hat{v})^\top$ is the expected displace-
 137 ment computed by fitting an affine motion model to the displacements of N_e
 138 neighboring moving features weighted by their distance to the feature (we
 139 used $N_e = 5$ in our experiment).

140 In (4), β is a positive constant (we use 1.0 in our experiments.) This num-
 141 ber can be set according to computational load and computational power;
 142 that is, the higher the available computational power, the smaller β should
 143 be set. λ is a smoothing term which we set to $\lambda = \sigma^2$.

144 The problem of minimizing $C = C_{LK} + \lambda C_{HS}$ can be solved using Jacobi
 145 iterations [5]. The JLK algorithm is more time consuming (usually 5-10 times
 146 slower than KLT), but with the help from neighboring moving features, the
 147 tracked feature points are less likely to merge or mix with scene features. The
 148 proposed SFHM method makes the tracking algorithm more robust while
 149 maintaining similar processing speed compared to KLT. More sample frames
 150 and their corresponding SFHMs and outputs from the classifier are shown in
 151 Figure 5.

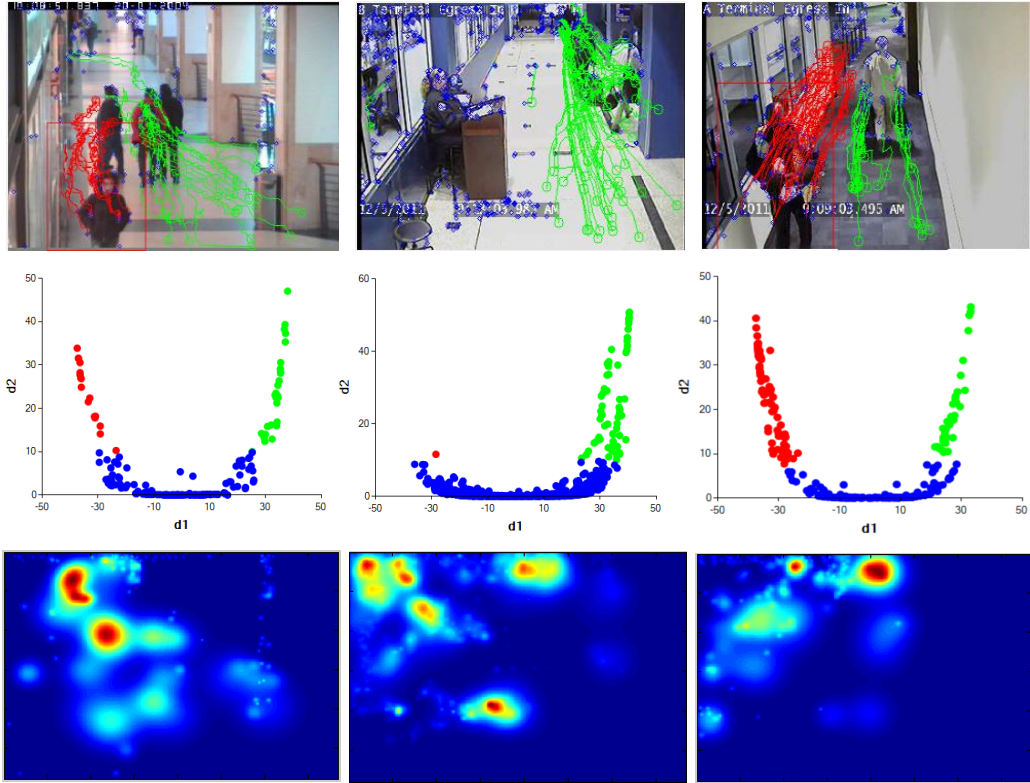


Figure 5: Classifier output and Scene Feature Heat Map for typical frames. The first row shows the frames processed with tracklets. The second row shows the output of the three-way classifier. The third row shows the corresponding Scene Feature Heat Map.

152 Features are tracked for every frame and are classified after a certain
 153 interval depending on the frame rate of the camera. Tracklets classified as
 154 counterflow are considered as potential alarms. Detection is finalized after
 155 an additional criterion. We found that most of the false alarms are caused by
 156 mixing tracks. Even with the three-way classifier, some of the mixed tracks
 157 are hard to filter since some regions contain both scene features and humans.
 158 However, the trajectories of mixed tracks are usually highly random. The

159 correlations between x and y coordinates are significantly lower than those
160 of other trajectories. By setting a threshold (we used 0.5 in our experiments)
161 on the correlation for trajectories, most false alarms caused by mixing point
162 tracks can be eliminated.

163 **6. Joint Processing in a Camera Network**

164 In most cases, the configuration/floor plan of the camera surveillance
165 network is known, which can be leveraged to further reduce the false positive
166 rate. Even though all the cameras may not share overlapping fields of view,
167 they generally cover the same path, which usually means that counterflow
168 should be detected in more than one camera. The design of the joint decision
169 mechanism depends on the physical setup of the camera network, as discussed
170 further in the next section.

171 **7. Experiments**

172 We evaluated our algorithms on several datasets, both standard ones and
173 custom-collected video at a large US airport (Cleveland-Hopkins Interna-
174 tional).

175 *7.1. CAVIAR*

176 First, we tested our algorithms on the standard CAVIAR dataset (clips
177 from a shopping center in Portugal) [11]. 27 video sequences from the corridor
178 view were used in the experiments, in which *WalkByShop1cor*, *2LeaveShop1cor*
179 and *2LeaveShop2cor* were used to train the classifier.

180 The other 24 sequences were tested with and without our scene-feature
181 based algorithm. As a baseline, we compare the results against a classifier

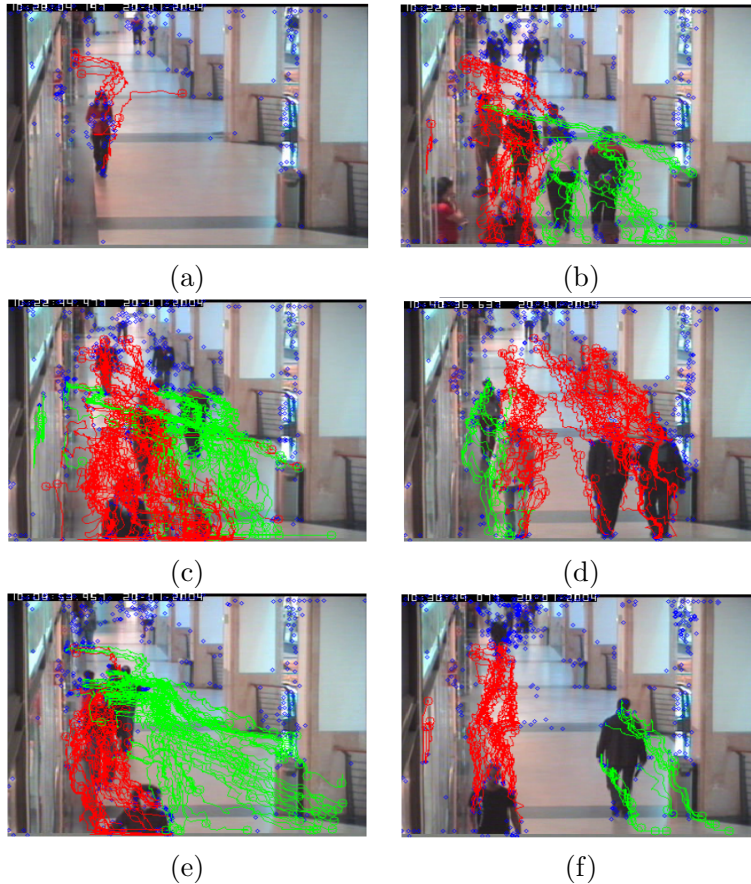


Figure 6: Sample images from CAVIAR with annotated results.

182 that only discriminates between normal flow and counterflow using the d_1
 183 feature (i.e., not taking into account scene features). We also compared the
 184 results against the algorithms of LPD [1] and LCSS [9]. The results are shown
 185 in Figure 7. Several examples are shown in Figure 6. Normal trajectories are
 186 displayed in green while counterflow trajectories are displayed in red.

187 Since LCSS is based on a similar feature tracking approach, its perfor-
 188 mance is similar to the 2-class baseline approach; its false alarm rate is

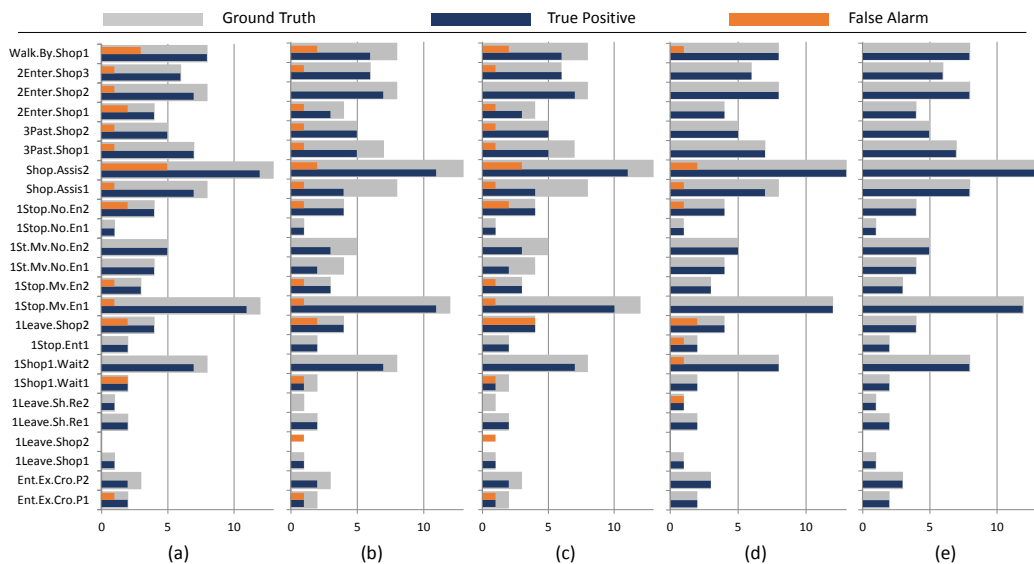


Figure 7: Results of the counterflow experiment on CAVIAR. (a) LPD[1]. (b) LCSS[9]. (c) 2-class classifier. (d) 3-class classifier. (e) 3-class classifier plus SFHM.

189 slightly better since the trajectory clustering in LCSS can bypass some mix-
 190 of-track trajectories. The LPD algorithm is based on a flow field that does
 191 not rely on trajectories. Its true positive rate is significantly higher than
 192 LCSS and the 2-class baseline approach. On the other hand, it is more sen-
 193 sitive to noise, resulting in a higher false positive rate. From the results we
 194 can see that with the 3-way classifier, the detection rate has been improved
 195 over the 2-class baseline from 79% to 99%, while the false positive rate has
 196 been reduced from 19% to 8%. The performance of the 3-way classifier sur-
 197 passes LPD and LCSS on both the true positive rate and false alarm rate.
 198 When adding the SFHM, the detection rate reaches 100% without any false
 199 positives.

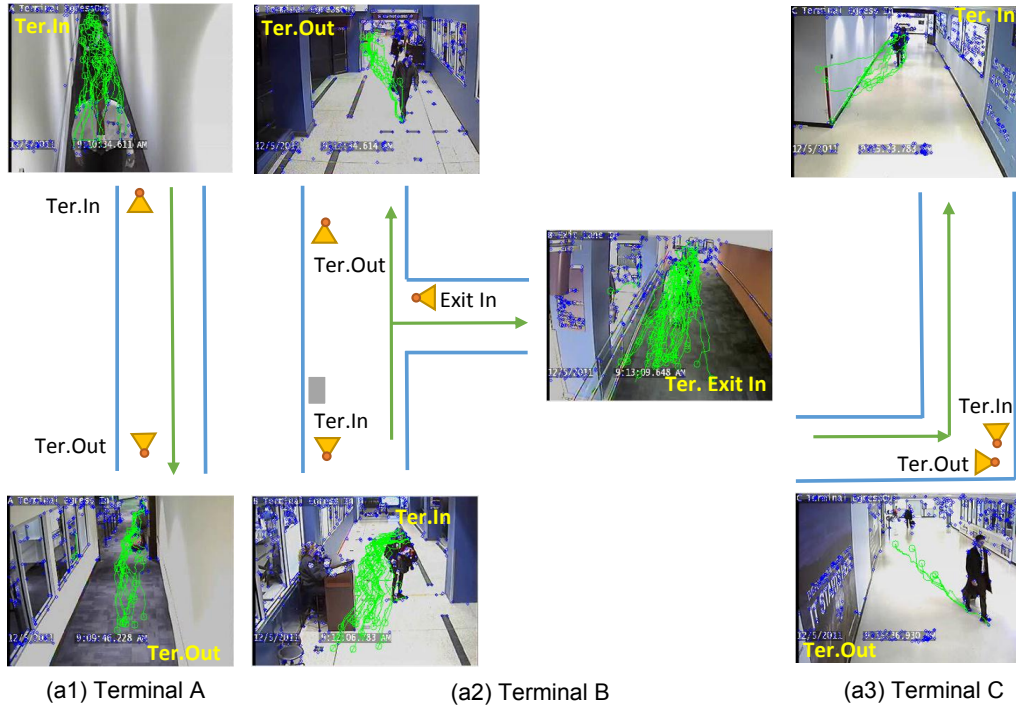
Table 1: Results of the counterflow experiment on the short airport videos. **GT** denotes the number of ground truth counterflows, **TP** the number of true positives and **FA** the number of false alarms.

Video	Len min	GT	LPD[1]		LCSS[9]		2-Class		3-Class		+SFHM	
			TP	FA	TP	FA	TP	FA	TP	FA	TP	FA
TA Eg.In	40	1	1	2	1	2	1	2	1	0	1	0
TA Eg.Out	32	2	2	6	2	6	2	6	2	1	2	0
TB Eg.In	40	10	8	4	9	4	8	4	10	1	10	0
TB Eg.Out	32	10	10	12	7	10	6	12	10	6	10	0
TC Eg.In	5	0	0	5	0	3	0	3	0	0	0	0
TC Eg.Out	5	2	2	6	0	5	0	5	2	3	2	0
Total	154	25	23	35	19	30	18	32	25	11	25	0

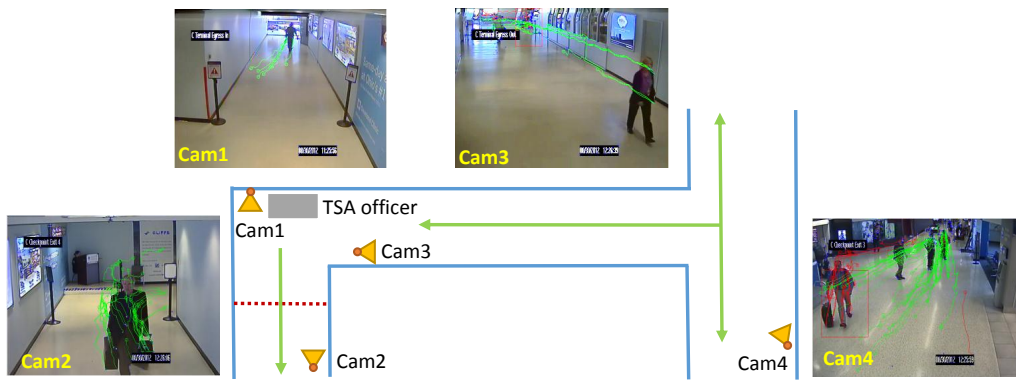
200 *7.2. Shorter Airport Videos*

201 We next tested the counterflow detection algorithm on six video sequences
 202 from cameras overlooking exit lanes at an airport. Figure 8(a) illustrates the
 203 configuration of the cameras and sample images. The classifier is first trained
 204 with a one-minute portion of the video and tested with the rest. The results
 205 for the six sequences are collected in Table 1, and several examples of normal
 206 flow and counterflow are shown in Figure 9. A bounding box corresponding
 207 to each suspicious target is also created.

208 These videos are all at low resolution (320×240) and contain periodic
 209 jitter. It can be seen that with the help of the 3-way classifier, the detection
 210 rate improved from 72% to 100% while the false positive rate was reduced
 211 from 64% to 30%. The performance of LPD and LCSS reflects the same
 212 conclusions from the CAVIAR experiment. Again, the performance of 3-
 213 way classifier surpasses both LPD and LCSS. When adding the SFHM, the
 214 algorithm achieved a 100% detection rate without any false alarms. No



(a) Floor plan and sample frames for Shorter Airport Videos



(b) Floor plan and sample frames for Long Airport Videos

Figure 8: Floor plans and sample frames from each camera.

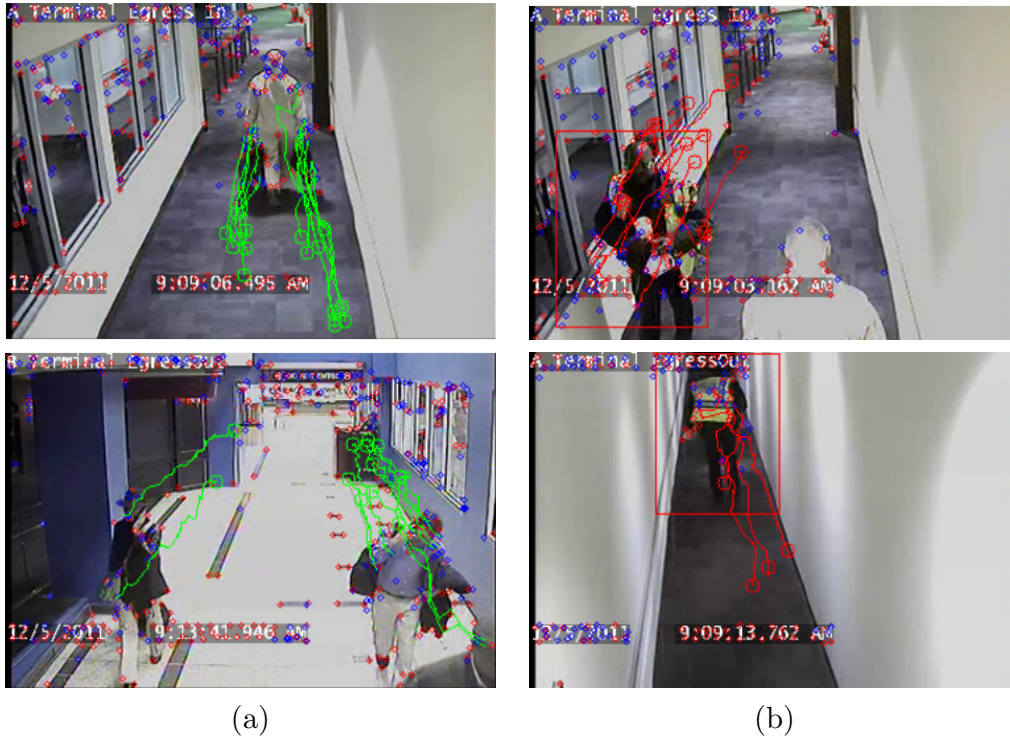


Figure 9: Sample flow classification results. (a) Normal flow. (b) Counterflow is detected and the target is located.

215 counterflow events were missed using the 3-way classifier.

216 7.3. Long Airport Videos

217 Finally, we conducted a long-term experiment at the airport with a cam-
 218 era network consisting of 4 cameras, as illustrated in Figure 8(b).

219 These cameras are at higher resolution (640×480). However, flicker and
 220 artifacts due to compression and illumination problems still make the task
 221 challenging, especially for 24/7 continuous processing. We trained the clas-
 222 sifier for each camera for 10 minutes. For this experiment, we also evaluated

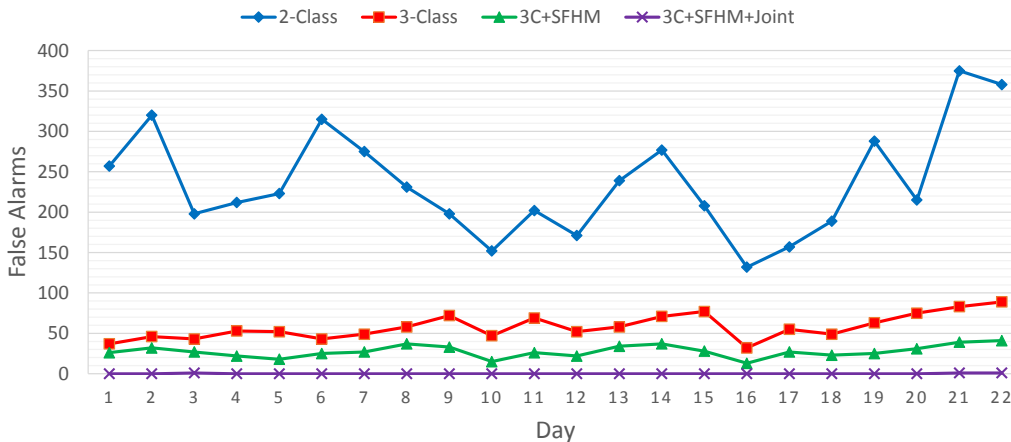


Figure 10: False alarms for the counterflow experiments on the long airport videos. There were 249 ground truth events, 234 of which were detected by the 2-class classifier, and all of which were detected by the other variants of the algorithm.

223 the method of relating results from multiple cameras mentioned in Section 6.
 224 We consider a counterflow event to be detected only if detections are found
 225 in both camera 1 and 2 or in both camera 1 and 3 within a 30 second time
 226 span (without requiring the detections to be found at exactly the same time).
 227 This time span can be set by the expected or statistically longest time for a
 228 person to walk from the FOV of camera 2 to the FOV of camera 3. How-
 229 ever, a detection found in camera 1 with high confidence (i.e., more than 3
 230 counterflow point tracks are found) is directly considered as a true detection
 231 since this viewpoint is most reliable. We processed video from 22 straight
 232 days from these 4 cameras in real time. Each day, about 10 counterflow
 233 events were generated by airport security officers to test the algorithm. The
 234 results are summarized in Figure 10.

235 From the results we can see that with the help of the 3-way classifier, the

236 detection rate improved from 93% to 100% while the false positive rate was
237 reduced from 96% to 83%. The addition of the SFHM further reduces the
238 false positive rate to 71%, which is still much too high. By jointly relating
239 the results from three cameras, the false positive rate was reduced to about
240 1%, which is considered to be operationally acceptable from the perspective
241 of airport security officers (less than 1 false alarm per day). No counterflow
242 events were missed using the 3-way classifier.

243 *7.4. Failure Cases*

244 The proposed algorithms may fail when processing videos with a highly
245 dynamic background, or that contain serious ghosting or compression arti-
246 facts. In our experiments, most of the false alarms are due to noise, jitter
247 or mixing point tracks. Since false alarms are easy to assess and discard,
248 the level of performance seems acceptable in practical applications given the
249 lengths of the videos involved. Some videos with false alarms are partic-
250 ularly challenging due to unusual walking patterns of passengers, “accept-
251 able” counterflow caused by security officers, mixing feature tracks, a com-
252 plex background, and passengers coming from an exit far from the camera.

253 **8. Conclusion**

254 As desired, the algorithms successfully detected all the counterflow oc-
255 currences in all the sequences without error. More importantly, the number
256 of false alarms has been significantly reduced by successive refinements to
257 the algorithm.

258 Both the false alarm rate and true positive rate are improved by the
259 proposed scene-feature-based algorithms. Experimental results show that the

260 proposed algorithms outperform LPD [1] and LCSS [9] on both a standard
261 dataset and real-world video sequences, suggesting that with the help of scene
262 features, trajectory-based counterflow detection approach can be significantly
263 improved. Future work includes improving the 3-way classifier so that it can
264 be trained without supervision, adding robust broken tracklet re-connection
265 to the algorithm, and identifying security officers and ignoring counterflows
266 caused by them.

267 **9. Acknowledgment**

268 This material is based upon work supported by the U.S. Department of
269 Homeland Security under Award Number 2008-ST-061-ED0001. The views
270 and conclusions contained in this document are those of the authors and
271 should not be interpreted as necessarily representing the official policies, ei-
272 ther expressed or implied of the U.S. Department of Homeland Security.
273 Thanks to Edward Hertelendy and Michael Young for supplying the data in
274 Section 7.

275 **References**

- 276 [1] S. Ali, M. Shah, A Lagrangian Particle Dynamics Approach for Crowd
277 Flow Segmentation and Stability Analysis, in: IEEE Conference on
278 Computer Vision and Pattern Recognition(2007).
- 279 [2] J. Alon, S. Sclaroff, G. Kollios, V. Pavlovic, Discovering clusters in mo-
280 tion time-series data, in: IEEE Conference on Computer Vision and
281 Pattern Recognition(2003).

- 282 [3] E. Andrade, S. Blunsden, R. Fisher, Modelling Crowd Scenes for
283 Event Detection, in: 18th International Conference on Pattern Recog-
284 nition(2006).
- 285 [4] G. Antonini, J. Thiran, Counting Pedestrians in Video Sequences Using
286 Trajectory Clustering, IEEE Transactions on Circuits and Systems for
287 Video Technology 16 (2006) 1008–1020.
- 288 [5] S.T. Birchfield, S.J. Pundlik, Joint tracking of features and edges, in:
289 IEEE Conference on Computer Vision and Pattern Recognition(2008).
- 290 [6] J.Y. Bouguet, Pyramidal Implementation of the Lucas Kanade Feature
291 Tracker Description of the algorithm, Technical Report, Microprocessor
292 Research Labs, Intel Corporation, 2002.
- 293 [7] G. Brostow, R. Cipolla, Unsupervised Bayesian Detection of Indepen-
294 dent Motion in Crowds, in: IEEE Conference on Computer Vision and
295 Pattern Recognition(2006).
- 296 [8] D. Buzan, S. Sclaroff, G. Kollios, Extraction and clustering of motion
297 trajectories in video, in: Proceedings of the 17th International Confer-
298 ence on Pattern Recognition(2004).
- 299 [9] A. Cheriyyadat, R. Radke, Detecting Dominant Motions in Dense
300 Crowds, IEEE Journal of Selected Topics in Signal Processing 2 (2008)
301 568–581.
- 302 [10] A.M. Cheriyyadat, R.J. Radke, Non-negative matrix factorization of par-
303 tial track data for motion segmentation, in: IEEE International Confer-
304 ence on Computer Vision(2009).

- 305 [11] EC Funded CAVIAR project/IST 2001 37540, Clips from Shopping Cen-
306 ter in Portugal, 2004.
- 307 [12] B.K. Horn, B.G. Schunck, Determining optical flow, *Artificial Intelli-*
308 *gence* 17 (1981) 185–203.
- 309 [13] I. Junejo, O. Javed, M. Shah, Multi feature path modeling for video
310 surveillance, in: 17th International Conference on Pattern Recogni-
311 tion(2004).
- 312 [14] B. Lucas, T. Kanade, An iterative image registration technique with an
313 application to stereo vision, *Proceedings of the 7th International Joint*
314 *Conference on Artificial Intelligence* (1981) 674–679.
- 315 [15] L. Marcenaro, G. Vernazza, Image stabilization algorithms for video-
316 surveillance applications, *International Conference on Image Processing*
317 (2001).
- 318 [16] E. Rosten, R. Porter, T. Drummond, Faster and better: a machine
319 learning approach to corner detection., *IEEE Transactions on Pattern*
320 *Analysis and Machine Intelligence* 32 (2010) 105–19.
- 321 [17] P.H. Tu, J. Rittscher, Crowd Segmentation Through Emergent Labeling,
322 *Lecture Notes in Computer Science* 3247 (2004) 187–198.
- 323 [18] Z. Wu, R.J. Radke, Using scene features to improve wide-area video
324 surveillance, in: *IEEE International Workshop on Camera Networks*
325 *and Wide Area Scene Analysis* (2012).